Consequences of Molecular-Level Ca^{2+} Channel and Synaptic Vesicle Colocalization for the Ca^{2+} Microdomain and Neurotransmitter Exocytosis: A Monte Carlo Study

Vahid Shahrezaei* and Kerry R. Delaney†
Departments of *Physics and †Biological Sciences, Simon Fraser University, Burnaby, British Columbia, Canada

ABSTRACT Morphological and biochemical studies indicate association between voltage-gated Ca^{2+} channels and the vesicle docking complex at vertebrate presynaptic active zones, which constrain the separation between some Ca^{2+} channels and vesicles to 20 nm or less. To address the effect of the precise geometrical relationship among the vesicles, the Ca^{2+} channel, and the proteins of the release machinery on neurotransmitter release, we developed a Monte Carlo simulation of Ca^{2+} diffusion and buffering with nanometer resolution. We find that the presence of a vesicle as a diffusion barrier alters the shape of the Ca^{2+} microdomain of a single Ca^{2+} channel around the vesicle. This effect is maximal in the vicinity of the vesicle and depends critically on the vesicle's distance from the plasmalemma. Ca^{2+}-sensor(s) for release would be exposed to markedly different [Ca^{2+}], varying by up to 13-fold, depending on their position around the vesicle. As a result, the precise position of Ca^{2+}-sensor(s) with respect to the vesicle and the channel can be critical to determining the release probability. Variation in the position of Ca^{2+}-sensor molecule(s) and their accessibility could be an important source of heterogeneity in vesicle release probability.

INTRODUCTION

Action potential-triggered release is distinguished from other types of cellular exocytosis by its fast on and off kinetics and its precise spatial localization (Matthews, 1996). It is known that neurotransmitter release requires high Ca^{2+} concentration ([Ca]) (Zucker, 1993), which can be achieved in close proximity to open Ca^{2+} channels, in ''Ca^{2+} microdomains'' (Chad and Eckert, 1984; Simon and Llinas, 1985; Zucker and Fogelson, 1986; Llinas et al., 1992). Ca^{2+}-driven vesicle fusion lags behind the influx of Ca^{2+} by a fraction of a millisecond (Llinas et al., 1981; Sabatini and Regehr, 1996) and terminates rapidly ($<$1–2 ms) after channel closure. These conditions require colocalization of Ca^{2+} channels and the Ca^{2+} sensor(s) of the release machinery in the nerve terminal to within $\sim$100 nm. Potential for even closer colocalization is now being established through both morphological and biochemical studies (Stanley, 1997). Freeze fracture studies in the frog neuromuscular junction have shown localization of large particles (some or all of which are thought to be Ca^{2+} channels) to the vesicle docking sites (Heuser et al., 1974; Pumplin et al., 1981). Some of these particles are within 20 nm from the point where docked vesicles contact the plasmalemma (Harlow et al., 2001; Stanley et al., 2003). Also, it is now widely accepted that N-type and P/Q-type Ca^{2+} channels, which are the predominant subtypes mediating release from presynaptic nerve terminals (Westenbroek et al., 1992; Westenbroek et al., 1995), can potentially couple physically to vesicle-associated proteins (syntaxin, synaptotagmin, and SNAP-25) (Sheng et al., 1998; Jarvis and Zamponi, 2001). The interactions between these proteins and the Ca^{2+} channel are Ca^{2+}-dependent and may regulate the activity of channels. Possibly, though, the more important role of these interactions is to constrain the position of the Ca^{2+} channel relative to the Ca^{2+}-sensor(s) for release.

Advances in the characterization of vesicle-associated proteins that are involved in exocytosis have greatly enhanced our understanding of neurotransmitter release (Sudhof, 1995). SNARE (soluble *N*-ethylmaleimide-sensitive factor attachment protein receptor) proteins of syntaxin, VAMP (also called synaptobrevin), and SNAP-25 are essential components of this machinery. Synaptic vesicles become ready for fusion when SNARE proteins on opposing membranes form a four-helix bundle (the so-called SNARE complex) that bring the membranes in close contact (Sutton et al., 1998; Weber et al., 1998). Among the proteins associated with synaptic vesicles, synaptotagmin is currently the best candidate for the Ca^{2+}-sensor mediating neurotransmitter release (Chapman, 2002). This is an abundant constituent of synaptic vesicles that binds up to five Ca^{2+} ions through two C2 domains (Ubach et al., 1998; Fernandez et al., 2001). Biochemical studies indicate that synaptotagmin undergoes Ca^{2+}-dependent interactions with a number of SNARE proteins and also membrane lipids, but which of these interactions are responsible for fast neurotransmitter release is not clear (Augustine, 2001). The cooperation of three-to-eight SNARE complexes may be needed for fusion (Hua and Scheller, 2001; Han et al., 2004). There is a synaptotagmin associated with each SNARE complex and their interactions play a role in fusion (Bai et al., 2004). So, there may be

Submitted March 26, 2004, and accepted for publication June 18, 2004.

Address reprint requests to V. Shahrezaei, Department of Physics, Simon Fraser University, 8888 University Dr., Burnaby, BC, Canada V5A 1S6. Tel.: 604-291-4395; Fax: 604-291-3592; E-mail: vshahrez@sfu.ca.

0006-3495/04/10/2352/13 $2.00

doi: 10.1529/biophysj.104.043380

numerous Ca^{2+} binding sites around the contact point of the vesicle and plasma membrane that need to bind Ca^{2+} to trigger release (Stewart et al., 2000).

Even though we are learning more about the molecular constituents of Ca^{2+}-triggered neurotransmitter release, we still do not have a widely accepted model for the Ca^{2+}-sensor sites. It is generally accepted that release is highly cooperative, and the cooperativity is functionally ~3–5 (Dodge and Rahamimoff, 1967; Heidelberger et al., 1994; Bollmann et al., 2000; Schneggenburger and Neher, 2000). For technical reasons the Ca^{2+} sensitivity of the Ca^{2+}-sensor has been determined for only a few synapses, yet the results have already revealed striking differences. For example, in goldfish retinal bipolar cells, the threshold for detectable release is above 20 μM (Heidelberger et al., 1994), whereas in the rat calyx of Held synapse this threshold is below 1 μM (Bollmann et al., 2000; Schneggenburger and Neher, 2000).

The present work is motivated by recent insights into the molecular and morphological aspects of neurotransmitter release. In particular, we are interested in the effect of active zone geometry on Ca^{2+} diffusion and accessibility of the Ca^{2+}-sensor to the Ca^{2+} source. It is known that obstacles can have significant effects on diffusion (Saxton, 1994; Olveczky and Verkman, 1998). For example, quantitative features of longitudinal diffusion of Ca^{2+} in retinal rod and cone outer segment cytoplasm reflects the anatomical structure of the outer segment, and it contributes to the differences in signal transduction between photoreceptor types (Nakatani et al., 2002; Andreucci et al., 2003; Holcman and Korenbrot, 2004). Since the Ca^{2+} channel, the vesicle, and the Ca^{2+}-sensor(s) of the release machinery are closely associated, we hypothesize that the presence of the vesicle could alter the shape of the Ca^{2+} microdomain and have significant effects on release. A thorough study of this issue demands simulations with nanometer resolution that are capable of retaining the essential features of the geometry of the active zone. We have achieved this by simulating the buffered diffusion of Ca^{2+} ions from the channel to the Ca^{2+}-sensor sites using a Monte Carlo scheme (Bartol et al., 1991). In this method, we simulate the random movement and reaction of individual Ca^{2+} ions and buffer molecules. This is computationally feasible, since the total number of Ca^{2+} ions coming in through each single Ca^{2+} channel is small (Stanley, 1993). We first study the effect of the vesicle as an obstacle to the free diffusion of Ca^{2+} from a single channel and the modifications it causes to the Ca^{2+} microdomain. Then, employing two representative release models, we look at the implications of the geometry on release, including the effect of the position of the Ca^{2+}-sensor(s) relative to the channel and the vesicle.

METHODS

Invasion of the nerve terminal by an action potential opens voltage-gated Ca^{2+} channels. Ca^{2+} ions rush in and diffuse within the nerve terminal, where they bind reversibly to fixed and mobile endogenous (or added exogenous) buffers via the reaction

$$Ca^{2+} + B \underset{k_{off}}{\overset{k_{on}}{\rightleftharpoons}} CaB, \tag{1}$$

where Ca^{2+} represents free calcium ions, B represents unbound buffer molecules, and CaB represents Ca^{2+} bound to buffer. Free Ca^{2+} ions can bind to the Ca^{2+}-sensor sites on the release machinery to initiate fusion of synaptic vesicles. Diffusion and reaction of Ca^{2+} and buffers can be studied by solving deterministic differential diffusion-reaction equations. These equations describe the spatial and temporal evolution of the Ca^{2+} and buffer concentrations ([Ca], [B], and [CaB]). For the buffer reaction (Eq. 1) with forward rate k_{on} and dissociation rate k_{off} the equations are (see e.g., Naraghi and Neher, 1997)

$$\begin{aligned}
\partial[Ca]/\partial t &= D_{Ca}\nabla^2[Ca] - k_{on}[Ca][B] + k_{off}[CaB] + I(t)\delta(r)\\
\partial[B]/\partial t &= D_{B}\nabla^2[B] - k_{on}[Ca][B] + k_{off}[CaB]\\
\partial[CaB]/\partial t &= D_{CaB}\nabla^2[CaB] + k_{on}[Ca][B] - k_{off}[CaB],
\end{aligned} \tag{2}$$

where D_{Ca}, D_B, and D_{CaB} are diffusion constants for Ca^{2+}, B, and CaB, respectively. $I(t)$ is the Ca^{2+} current and $\delta(r)$ is a Dirac delta function (assuming the channel is at the origin).

There is no exact analytical solution for the above partial differential equations due to their nonlinearity (the terms with order two in concentration). Consequently, one has to solve this set of equations numerically using the finite difference method in three spatial dimensions and time, given specific boundary conditions (Cooper et al., 1996; Meinrenken et al., 2002; Winslow et al., 1994; Yamada and Zucker, 1992). In the case of a single channel with a free boundary the problem will effectively be one-dimensional because of spherical symmetry. For two different limits one can simplify the diffusion-reaction equations further. First, if the reaction kinetics act on a timescale that is much faster than the timescale for diffusion, then one can assume a local equilibrium always exists for the reaction described by Eq. 1. This so-called fast buffer approximation reduces the set of Eq. 2 to a single differential equation, which has advantages for numerical and analytical analysis (Smith, 1996; Wagner and Keizer, 1994). The second approximation assumes that changes in free and bound buffer concentrations are negligible, which is valid for small amounts of Ca^{2+} entry in the presence of a large concentration of buffer. This allows for linearization of Eq. 2, which in turn makes an analytical analysis possible for the [Ca] steady-state condition (Stern, 1992). This has been generalized to the case where multiple buffer types are present (Naraghi and Neher, 1997).

The exact analytical results and approximate solutions provide useful insight into the effect of buffers. Fixed buffers prolong the approach to the [Ca] steady state but do not affect the final form of the Ca^{2+} microdomain. In contrast, mobile buffers make the [Ca] gradient steeper. A uniquely defined length-constant is associated with each mobile buffer, which is a measure of its capability to buffer Ca^{2+} close to the channel (Naraghi and Neher, 1997).

Monte Carlo scheme

Monte Carlo simulation is an alternative method to study reaction-diffusion problems. It has been used in the context of modeling neurotransmitter release in a number of studies (Bartol et al., 1991; Bennett et al., 2000a,b; Gil et al., 2000; Glavinovic and Rabie, 2001; Kennedy et al., 1999; Segura et al., 2000). There are three advantages inherent to the Monte Carlo approach compared to deterministic reaction-diffusion equations:

1. It is closer to the physical situation found in a system with small numbers of particles in the sense that it gives some indication of the stochastic fluctuations that are likely to occur.
2. The computational time does not grow steeply as the spatial resolution increases, which is the case with the numerical solution of the diffusion-reaction equation.
3. The boundary conditions of the system are easily taken into account and one can easily vary such conditions.

In the Monte Carlo simulation method, the motion of each individual molecule (Ca^{2+} or buffer) is followed as it diffuses inside the nerve terminal. This is not done at the level of actual Brownian motion, but rather at a coarser level, using random walk theory (e.g., see Raichl, 1980). The average distance traveled by a molecule (Δl) during the time interval Δt depends on the diffusion coefficient as

$$\Delta l = 2(D\Delta t/\pi)^{1/2}. \quad (3)$$

We are interested in the effect of the fine geometry of the active zone on release. To be able to resolve the steep concentration gradient close to the Ca^{2+} entry site and the diffusion obstacles, we need to use a Δl comparable to the length scale of the geometry of the system, which is approximately a nanometer. The time step between successive movements of the particles is related to Δl (Eq. 3) and as a result is of the order of 10 ns. So a millisecond of the simulation of the system takes $\sim 10^5$ Monte Carlo steps. Although the small time step and long computation time are the price that we pay for high spatial resolution, it also pays in simplification of the treatment of the Ca^{2+}-buffer reactions as we describe later. We begin our Monte Carlo simulation by assigning random positions to the molecules in the simulation box. Then, in each time interval, we repeat the following steps:

1. Introduce a new Ca^{2+} ion into the system at the channel mouth with probability $I(t)\Delta t/(2e)$, where e is the charge of electron ($2e$ is the charge of Ca^{2+}). This probability is much smaller than unity.
2. Update the positions of all molecules by adding a random vector to the position of each molecule. The components of this vector were chosen from a Gaussian distribution centered around zero with a standard deviation of $(2D\Delta t)^{1/2}$. For buffer molecules (bound or free), the diffusion coefficient is much smaller than the Ca^{2+} diffusion coefficient, so we update their position once every D_{Ca}/D_B time steps to save computation time. With the values used for D_{Ca} and D_B the ratio is an integer.
3. Check the boundary condition for each molecule and modify their position accordingly; boundary conditions are explained in the next section.
4. Any Ca^{2+}/free buffer pair that is closer than a certain distance (r_{int}) bind to each other with probability p_{on}, which depends on the forward rate of reaction as

$$p_{on} = k_{on}\Delta t/(^4/_3\pi N_A r_{int}^3), \quad (4)$$

   where N_A is Avogadro's number.
5. Any bound buffer can dissociate to Ca^{2+} and free buffer with probability

$$p_{off} = k_{off}\Delta t. \quad (5)$$

The particular form for p_{on} and p_{off} in Eqs. 4 and 5 is chosen to produce the same equilibrium ratios of [Ca], [B], and [CaB] as predicted by the deterministic reaction expressions in Eq. 2. In a given system with volume V, the change in the number of CaB molecules (N_{CaB}) in a small time interval of Δt is

$$\Delta N_{CaB} = (k_{on}[Ca][B] - k_{off}[CaB])\Delta t V N_A$$
$$= k_{on}\Delta t N_{Ca} N_B/(VN_A) - k_{off}\Delta t N_{CaB}, \quad (6)$$

where N_{Ca} and N_B are the number of Ca^{2+} ions and buffer molecules, respectively. Here, we have assumed a constant concentration for each molecule throughout V. In the Monte Carlo simulation the change in N_{CaB} in each time step is equal to the number of new interactions between Ca^{2+} ions and buffer molecules minus the number of CaB molecules that dissociate. So, we have

$$\Delta N_{CaB} = p_{on} N_{Ca} N_B V_{int}/V - p_{off} N_{CaB}. \quad (7)$$

The chance that a Ca^{2+} ion is within the interaction distance (r_{int}) from a buffer molecule is proportional to N_B and the ratio of the interaction volume ($V_{int} = 4/3\pi r_{int}^3$) to the total volume of the system V. By equating first and second terms of Eqs. 6 and 7 one can derive the expressions given in Eqs. 4 and 5. This derivation relies on the fact that Δt is sufficiently small. We performed some control simulations (data not shown) to ensure that our choice of Δt satisfied this condition.

Because of the stochastic nature of this method, repeated trials must be performed to assess the average behavior of the system. This is a disadvantage of the Monte Carlo method, when one needs to examine the average behavior of the system. Sometimes thousands of trials are needed to obtain reasonable averages, which in turn can be computationally expensive. Since in most of this study, we are interested in the steady-state profile of [Ca] the averaging can be done more efficiently. Instead of running the simulation each time from the beginning, we average over a fraction of millisecond after the steady state is achieved. The steady-state concentration profiles in this study are the result of averages over 0.2 ms of 500 Monte Carlo runs. That makes $\sim 10^7$ independent samplings.

To avoid correlated sequences and therefore systematic errors when averaging Monte Carlo trials, the proper choice of random number generator is important. We used the Mersenne Twister random number generator algorithm, which is computationally efficient and has an exceptionally long period (Matsumoto and Nishimura, 1998).

All the programming was done in ''C.'' We ran the simulations on Simon Fraser University's Beowulf cluster. The isoconcentration surfaces in Fig. 3 were produced using MATLAB.

Geometry and the parameters

The simulation volume comprised a rectangular cubic box of size $L \times L \times L/2$ with the Ca^{2+} channel situated at the center of one of the square sides, as shown in Fig. 1. The channel side (x,y plane in Fig. 1 *A*) is reflective to Ca^{2+} to mimic the plasma membrane; all other sides of the box are free for Ca^{2+} diffusion. Free Ca^{2+} ions will disappear if they pass through free boundaries (this is also called the absorbing boundary condition). Because in reality some Ca^{2+} ions come back to the system, the absorbing boundary condition is an approximation. The [Ca] close to the boundary decays to zero but the effect on [Ca] far from the boundary is negligible. All the boundaries are reflective for buffers (free or bound). This choice of boundary conditions can approximate a Ca^{2+} source in an infinite space filled with a constant concentration of buffer but it is not exact, since the total amount of buffer is finite and will saturate at very long times. Since we are interested in short times (<1 ms) and Ca^{2+} dynamics close to the channel (<100 nm) these prove to be reasonable approximations.

We positioned a docked synaptic vesicle at a distance d from the channel (d is defined as the distance from the channel to the projection of the center of the vesicle on the presynaptic plasmalemma as shown in Fig. 1 *B*). Based on morphological and biochemical data, a reasonable distance for the closest channel to the vesicle is ~20 nm (Bennett et al., 1997; Harlow et al., 2001; Stanley et al., 2003). The distance between the vesicle and the plasma membrane is h (Fig. 1 *B*). Based on the speed of synaptic fusion and the EM

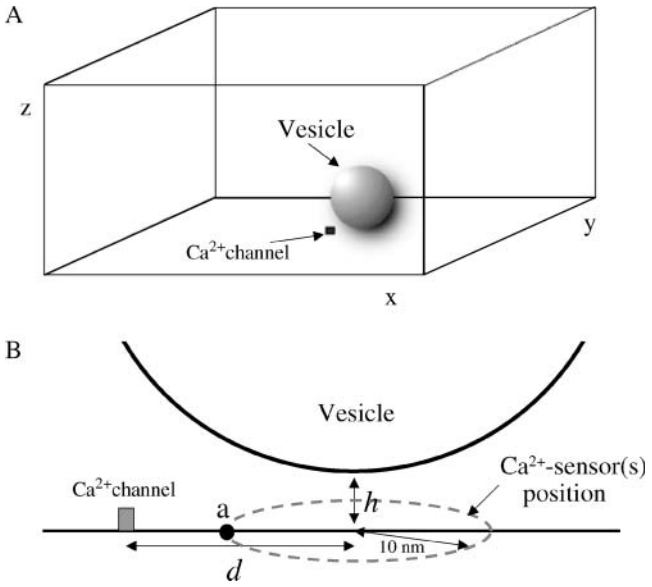

FIGURE 1 (*A*) Schematic view of simulation box, Ca^{2+} channel, and vesicle. (*B*) Cross sectional view of the arrangement of the channel and vesicle (parallel to the *x*,*z* plane in *A*). *d* and *h* are channel-vesicle and vesicle-membrane separations, respectively. Dashed circle with a radius of 10 nm (on the *x*,*y* plane in *A*) indicates the potential positions for the Ca^{2+}-sensor site(s).

studies, we posit *h* cannot be more than a few nanometers at most. We chose *h* to be zero for the most of our simulations and explored the effect of increasing *h* up to 50 nm. The vesicle acts as an obstacle to diffusion, so the boundary condition on the vesicle for the Ca^{2+} and buffers is reflective.

We do not consider any mechanisms for Ca^{2+} extrusion through the membrane, since their contribution to Ca^{2+} concentration profiles for time intervals of <1 ms will be irrelevant (Sala and Hernandez-Cruz, 1990). Also, for similar reasons, we do not consider any sequestration and release from internal stores. We only consider the presence of a mobile endogenous buffer. As discussed above, fixed buffers are less effective in affecting the Ca^{2+} microdomain, since they do not contribute to the steady-state [Ca] profile due to rapid saturation. We considered an endogenous buffer with a rather high affinity (dissociation constant, $K_d = K_{off}/K_{on} = 2\ \mu M$), fast kinetics ($K_{on} = 3 \times 10^8\ M^{-1}\ s^{-1}$), and slow diffusion ($D_B = D_{CaB} = 27.5\ \mu m^2\ s^{-1}$) (Burrone et al., 2002). We use 0.5 mM concentration of this buffer, which is equivalent to a buffer capacity ($[B]_{total}/K_d$) of 250. Buffer capacity is a measure of the ratio of equilibrium of bound Ca^{2+} to free Ca^{2+} at low [Ca].

For the single-channel Ca^{2+} current, we use a square wave form, with a height of 0.3 pA and a width of 0.3 ms. This is equivalent to ~300 Ca^{2+} ions, which is close to estimates for the influx through a single channel resulting from a single action potential in the presynaptic calyx terminal synapsing onto the ciliary ganglion cell of the chick (Stanley, 1993). The release is not very sensitive to the exact form of the Ca^{2+} current (see Results) and that justifies the simple wave form used in the study. All the simulation parameters are summarized in Table 1.

Release model

A large variety of Ca^{2+}-triggered release models have been suggested by experiments and employed in modeling studies. Here we compare a low-affinity and a high-affinity model for Ca^{2+} binding to the release-triggering site. The low-affinity model is derived from experiments using flash photolysis of caged Ca^{2+} in the goldfish retinal bipolar synapse

TABLE 1 Summary of parameters used in the Monte Carlo simulation

Geometrical parameters	
Size of the box	$L = 400$ nm
Vesicle radius	$R = 25$ nm
Channel vesicle distance	$D = 20$ nm
Ca channel	
Current	$I_{Ca} = 0.3$ pA
Channel opening time	$t_{Ca} = 0.3$ ms
Buffers (mobile)	
Concentration	[B] = 0.5 mM
Forward rate	$k_{on} = 3 \times 10^8\ M^{-1}\ s^{-1}$
Dissociation rate	$k_{off} = 600\ s^{-1}$
Diffusion	
Calcium diffusion coefficient	$D_{Ca} = 220\ \mu M^2\ s^{-1}$
Buffer diffusion coefficient	$D_B = D_{CaB} = 27.5\ \mu M^2\ s^{-1}$
Monte Carlo parameters	
Time step	$\Delta t = 10.2$ ns
Average jump size in each coordinate	$\Delta l = 1.69$ nm
Interaction range	$r_{int} = 2$ nm
Release model 1	
Forward rate	$k_{on} = 1.4 \times 10^6\ M^{-1}\ s^{-1}$
Dissociation rate	$k_{off} = 2000\ s^{-1}$
Cooperative factor	$b = 0.4$
Fusion rate	$\rho = 3000\ s^{-1}$
Release model 2	
Forward rate	$k_{on} = 3 \times 10^8\ M^{-1}\ s^{-1}$
Dissociation rate	$k_{off} = 3000\ s^{-1}$
Forward fusion intermediate	$\gamma = 30{,}000\ s^{-1}$
Backward fusion intermediate	$\delta = 8000\ s^{-1}$
Fusion rate	$\rho = 40{,}000\ s^{-1}$

(Heidelberger et al., 1994). It has four cooperative Ca^{2+}-sensor sites and a final Ca^{2+}-independent fusion step. The scheme of this model is

$$X \underset{k_{off}}{\overset{4k_{on}[Ca]}{\rightleftharpoons}} XCa_1 \underset{2bk_{off}}{\overset{3k_{on}[Ca]}{\rightleftharpoons}} XCa_2 \underset{3b^2k_{off}}{\overset{2k_{on}[Ca]}{\rightleftharpoons}} XCa_3 \times \underset{4b^3k_{off}}{\overset{k_{on}[Ca]}{\rightleftharpoons}} XCa_4 \overset{\rho}{\rightarrow} F, \quad (8)$$

where *b* is the cooperativity factor and ρ is the rate of the fusion process. The cooperativity factor introduces chemical cooperativity between the binding sites, so the dissociation rates (and resulting dissociation constants) for the second, third, and fourth Ca^{2+} ion will be reduced with respect to the first by a factor of *b*, b^2, and b^3 (*b* is <1 in this model).

The high affinity model that we use is from a similar study of the calyx of Held synapse (Bollmann et al., 2000). It has five independent Ca^{2+}-sensor sites and two Ca^{2+}-independent fusion steps,

$$X \underset{k_{off}}{\overset{5k_{on}[Ca]}{\rightleftharpoons}} XCa_1 \underset{2k_{off}}{\overset{4k_{on}[Ca]}{\rightleftharpoons}} XCa_2 \underset{3k_{off}}{\overset{3k_{on}[Ca]}{\rightleftharpoons}} XCa_3 \times \underset{4k_{off}}{\overset{2k_{on}[Ca]}{\rightleftharpoons}} XCa_4 \underset{5k_{off}}{\overset{k_{on}[Ca]}{\rightleftharpoons}} XCa_5 \underset{\delta}{\overset{\gamma}{\rightleftharpoons}} XCa_5^* \overset{\rho}{\rightarrow} F, \quad (9)$$

where XCa_5^* is an intermediate state before fusion. The values of the forward and dissociation rates and fusion parameters for both models are given in Table 1.

The actual position of the Ca^{2+}-sensor(s) relative to the Ca^{2+} channel and the vesicle is not known. If one assumes that the vesicle and the presynaptic membrane are tightly pressed together at the center, then there is

a little space for the proteins there. We therefore assume the Ca^{2+} binding sites are somewhere around the vesicle, close to the membrane, probably at an average distance of 10 nm around the contact point of the vesicle and the membrane.

RESULTS

The synaptic vesicle and [Ca] microdomain

It is well established that after the opening of the channel, [Ca] in the vicinity of its mouth reaches a steady state in few microseconds (Simon and Llinas, 1985). In our simulations, it takes 3 μs for [Ca] to reach 80% of its maximum at a distance of 10 nm from the channel (15 μs for a distance of 30 nm; see Fig. 2 *A*). Also, after channel closure, this standing [Ca] fades away in a few microseconds. Buffers (mobile or fixed) prolong the approach to steady state and delay the decay of the Ca^{2+} microdomain. Nonetheless, the timescales for the rise and fall of [Ca] are much faster than the average channel opening time ($\sim$1 ms), so release is mostly affected by steady-state [Ca]. To evaluate the steady-state properties we first look at the [Ca] gradients close to a single Ca^{2+} channel in the absence of any obstacle for diffusion. Fig. 2 *B* shows the steady-state [Ca] as a function of distance from the Ca^{2+} channel. Even though average [Ca] at the vicinity of an open channel reaches levels much higher than the basal level, it corresponds to very few Ca^{2+} ions. At steady state, the average number of Ca^{2+} ions within a radius of 10 or 30 nm is 0.18 or 1.23, respectively. Monte Carlo simulation results show that the number of Ca^{2+} ions found at a given moment of time in the vicinity of the channel fluctuates significantly (Bennett et al., 2000a). Within a radius of 10 nm most of the time there is no Ca^{2+} ion present; but intermittently several ions can be found. Since molecules are modeled individually in the Monte Carlo method, fluctuations in local concentration are automatically retained. With regard to this capability, we did not use the Monte Carlo method to its full capacity in this study, and only examined the average behavior of the system rather than the concentration fluctuations.

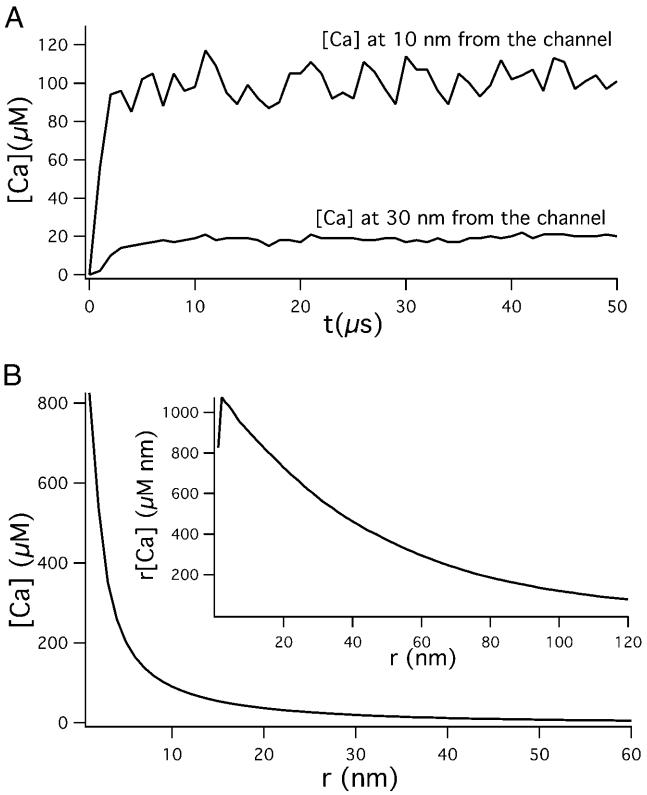

FIGURE 2 (*A*) [Ca] as a function of time at 10 nm and 30 nm away from the channel. Monte Carlo results shown are average of 10^5 runs. (*B*) [Ca] as a function of distance from the channel at 0.3 ms after sustained channel opening. Monte Carlo results shown are average of 10^8 runs. (*Inset*) From the same data the product of the *r* and [Ca] is shown in a wider range of distances, which fits well with a single exponential function with a length constant of 45 nm.

Steady-state [Ca] in the absence of mobile buffers has a $1/r$ form. Therefore, to look at the mobile buffer effect, we show the product of *r* and [Ca] in Fig. 2 *B* (*inset graph*). This product for distances $>$5 nm can be well described by a single exponential decay with a length constant of $\sim$45 nm. This is in good agreement with approximate solutions to diffusion reaction equations (Stern, 1992; Naraghi and Neher, 1997). Deviations for distances comparable to the average jump size ($\sim$1.69 nm) are expected, since the Monte Carlo method will fail to follow the steep gradient below its average jump size scale. These results suggest that despite large concentration fluctuations between different trials in the Monte Carlo simulation, the average behavior of the system can still be well described by the reaction-diffusion equations.

In the absence of any diffusion barrier, the [Ca] spatial profile will be spherically symmetric. So the [Ca] isoconcentration surfaces are concentric hemispheres around the Ca^{2+} channel. However, presynaptic terminals are not comprised of empty space. They contain many structural proteins and intracellular organelles. Most importantly, synaptic vesicles, that can be just a few tens of nanometers away from the channel mouth, may limit the free diffusion of Ca^{2+} and Ca^{2+} buffers (Kennedy et al., 1999; Tang et al., 2000; Glavinovic and Rabie, 2001). Using our Monte Carlo scheme, we investigate the effect of synaptic vesicle(s) on the steady-state [Ca] profile. Since the steady state will be reached quickly even in the presence of a vesicle, we focus our attention on standing Ca^{2+} microdomains.

First, we take the case of a single channel and a vesicle as shown in Fig. 1 ($h = 0$; for other parameters used, see Table 1). Fig. 3 shows the shape of the constant-[Ca] surface for two concentrations, [Ca] = 10 μM in *A* and [Ca] = 150 μM in *B*. The presence of the vesicle as a diffusion barrier for Ca^{2+} has a pronounced effect on the 10 μM surface (Fig. 3 *A*). The 150 μM surface is also not a complete hemisphere; and it is not centered at the channel but pushed toward the vesicle (Fig. 3 *B*).

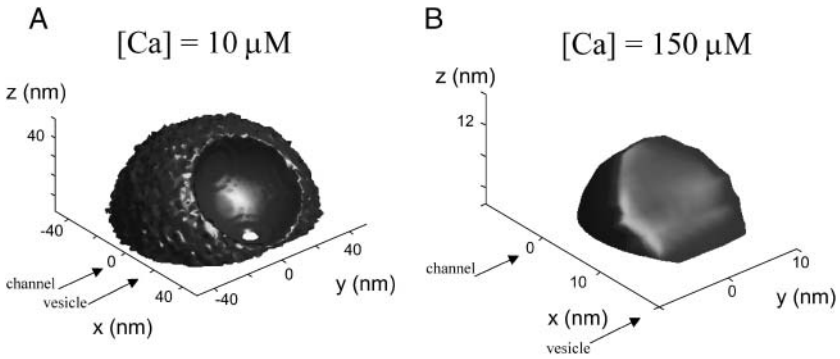

FIGURE 3 Ca^{2+} microdomain in the presence of the vesicle, at 0.3 ms after sustained opening of the channel. The isoconcentration surfaces are the result of interpolation of average [Ca] from Monte Carlo runs. (*A*) Constant concentration surface [Ca] = 10 μM. (*B*) Constant concentration surface [Ca] = 150 μM.

To gain further insight into the effects of a vesicle on free Ca^{2+} diffusion, we look at the two-dimensional cross sections of steady-state [Ca]. Fig. 4, *A* and *B*, show the image plots of [Ca] profile in two perpendicular cross sections of the system, one through the channel and the vesicle (*x*,*z* plane in Fig. 1 *A*) and the other parallel and close to the presynaptic plasmalemma (*x*,*y* plane in Fig. 1 *A*). The vesicle shapes the [Ca] profile in its vicinity. This is particularly evident when we look at the difference between these [Ca] profiles and the corresponding [Ca] profiles in the absence of a vesicle (Fig. 4, *C* and *D*). On the channel side of the vesicle, [Ca] reaches higher levels than when there is no vesicle (up to twofold). Correspondingly, on the other side of the vesicle, [Ca] will not reach levels as high as when there is no vesicle. These correspond, respectively, to the regions with positive and negative values in Fig. 4, *C* and *D*, and reflect blockage of free diffusion of Ca^{2+} by the vesicle. The vesicle reduces the escape routes for Ca^{2+} ions and thereby increases the effective distance from the channel to the other side of the vesicle. If we assume that the bottom of the vesicle is touching the presynaptic terminal membrane, then the closest that one can fit a protein between the vesicle and the membrane is ~10 nm from the center (see Discussion). The points around this circle have different distances from the channel (from 10 nm to 30 nm), so the standing [Ca] would be significantly different for these points. The presence of the vesicle magnifies this difference. Fig. 5 *A* shows [Ca] as a function of the angle around this circle. Zero degree corresponds to the closest point to the channel and 180° corresponds to the furthest point from the channel. With a vesicle present, [Ca] varies ~13-fold, from 16 μM to 207 μM, whereas this difference is only approximately fivefold in the absence of the vesicle. This observation implies that the position of the Ca^{2+} sensor around the vesicle relative to the Ca^{2+} channel could be extremely important to the likelihood of the sensor successfully binding Ca^{2+} to stimulate release. We will look at this issue in the next section.

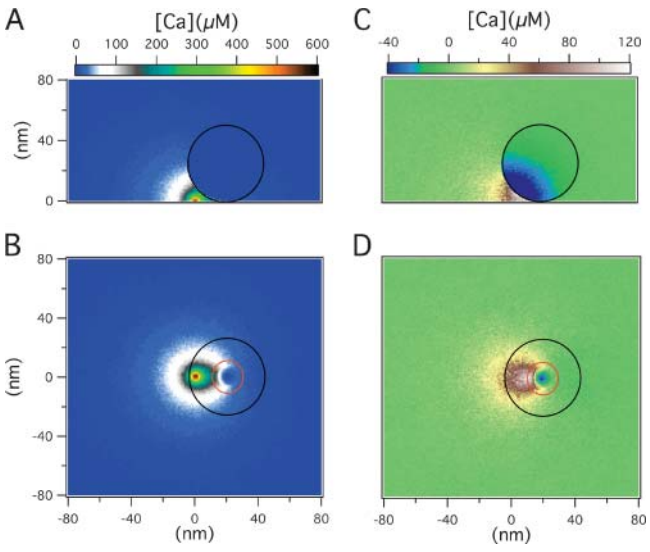

FIGURE 4 (*A*) The image plot of [Ca] in the plane $y = 0$ (*x*,*z* cross section of Fig. 1 *A*) after a sustained opening of the channel for 0.3 ms in the presence of the vesicle. (*B*) The image plot of [Ca] in the plane $z = 0$ (*x*,*y* cross section of Fig. 1 *A*) after a sustained opening of the channel for 0.3 ms in the presence of the vesicle. (*C*) [Ca] in the presence of the vesicle *A* minus [Ca] in the absence of the vesicle. (*D*) [Ca] in the presence of vesicle *B* minus [Ca] in the absence of the vesicle. The black circles in *B* and *D* are the projection of the vesicle on the membrane, whereas the red circles correspond to possible positions for the Ca^{2+}-sensor.

Due to the reflection of Ca^{2+} off the vesicle [Ca] 10 nm from the channel mouth, midway between the channel and the vesicle (point *a* in Fig. 1 *B*), is very similar to the Ca^{2+} transient at 5 nm from the channel in the absence of the vesicle. Fig. 5 *B* shows the actual and effective diffusional distance of the points around the vesicle from the channel. The effective diffusional distance for a point around the vesicle is defined to be the distance corresponding to the same steady-state [Ca] in the absence of vesicle. The presence of the vesicle changes the average path for a Ca^{2+} ion to reach different points. The effective diffusional distance will be reduced for the points on the channel side of the vesicle and will be increased for the points on the opposite side of the vesicle. This relationship is useful to relate one-dimensional solutions of the diffusion-reaction equations in spherical coordinates to the three-dimensional Monte Carlo results in the presence of the vesicle.

The blocking effect of a vesicle on Ca^{2+} diffusion is critically dependent on the vesicle-membrane distance *h*.

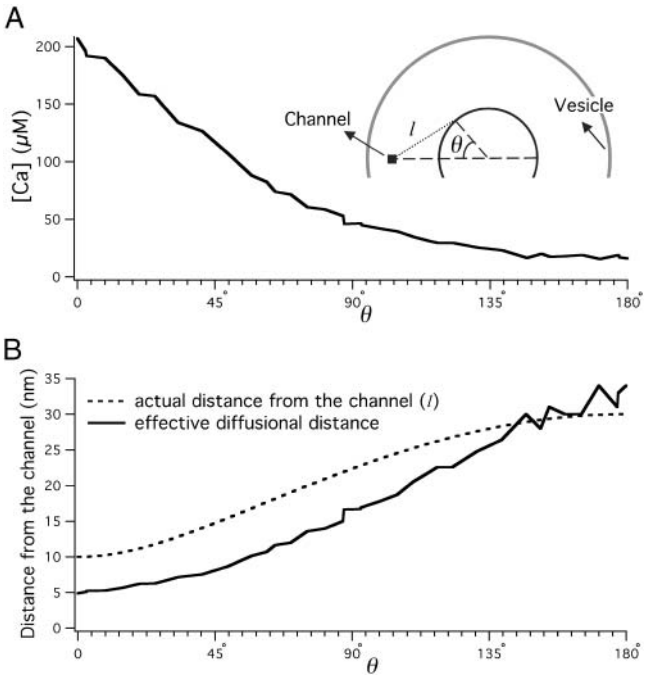

FIGURE 5 (*A*) [Ca] around the vesicle on a circle with radius of 10 nm as a function of angle with the line between the channel and vesicle. (*B*) The actual and effective distances from the channel to the points around the circle with radius of 10 nm as a function of angle with the line between the channel and vesicle. Actual distance is the geometrical distance from the point to the Ca^{2+} channel. The effective diffusional distance for a point around the vesicle is defined to be the distance corresponding to the same steady-state [Ca] in the absence of vesicle.

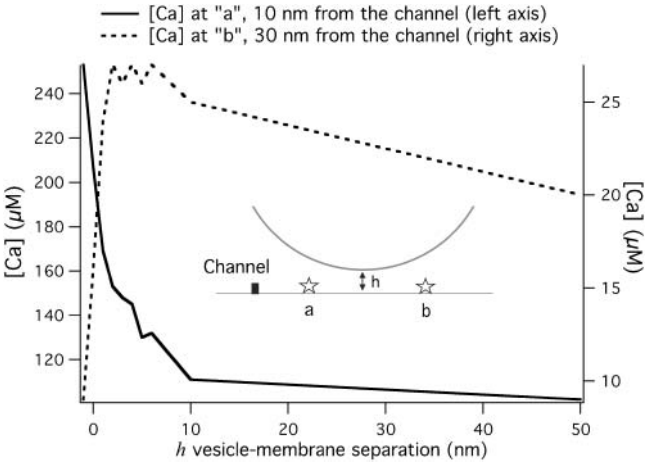

FIGURE 6 The steady-state [Ca] at 10 nm and 30 nm from the channel in the presence of the vesicle as a function of *h*, the distance from vesicle to membrane.

Fig. 6 explores a wide range of vesicle-membrane distances, from $h = -1$ nm where the vesicle has been pushed into the membrane, to very large $h = 50$ nm, where there is virtually no blocking effect. For the channel side of the vesicle (point *a* in Fig. 6), the average path for Ca^{2+} ions from the channel to a given point has been reduced, since some Ca^{2+} ions will bounce off the vesicle and reflect back. This effect disappears rapidly as the vesicle-membrane distance is increased. To the far side of the vesicle from the channel (point *b* in Fig. 6) there is a minimum average path at a distance *h* of ~3–5 nm. For smaller *h*-values, the Ca^{2+} ions have to go around the vesicle, so the standing [Ca] achieved is less than it would be without a vesicle. But, as *h* grows, the site on the other side of the vesicle becomes directly accessible to Ca^{2+} ions from the channel, and they can also bounce off the underside of the vesicle to access the far side. The [Ca] around the vesicle rapidly approaches the [Ca] values in the absence of the vesicle as *h* grows. The effect of the vesicle in modifying [Ca] is <20% for $h > 10$ nm. These results suggest docked vesicles will have a much greater effect on the [Ca] microdomain profile than nondocked vesicles.

The extent of the blocking effect of an obstacle on diffusion is dependent on its size, so a smaller vesicle is less effective in modifying the Ca^{2+}. For example, a docked vesicle ($h = 0$) with diameter of 30 nm, positioned 20 nm away from the channel, the steady-state [Ca] on the channel side of the vesicle reaches to ~135 μM. The [Ca] on the far side of the vesicle from the channel (point *b* in Fig. 6) reaches to ~18 μM. Using a simple planar geometry for the vesicle and assuming a Ca^{2+} channel is located right underneath the vesicle, a strong [Ca] dependence upon vesicle diameter was reported previously by Glavinovic and Rabie (2001). They suggested that larger vesicles have a higher probability of release due to the higher [Ca] levels achieved in their vicinity. This is in contrast to our results, for which a larger vesicle will increase the [Ca] on one side but decrease it on the other side.

In Fig. 7 we look at the effect of various channel-vesicle separations (*d*) on Ca^{2+} profile distortion in the vicinity of the channel or the vesicle. We look at the [Ca] at a point

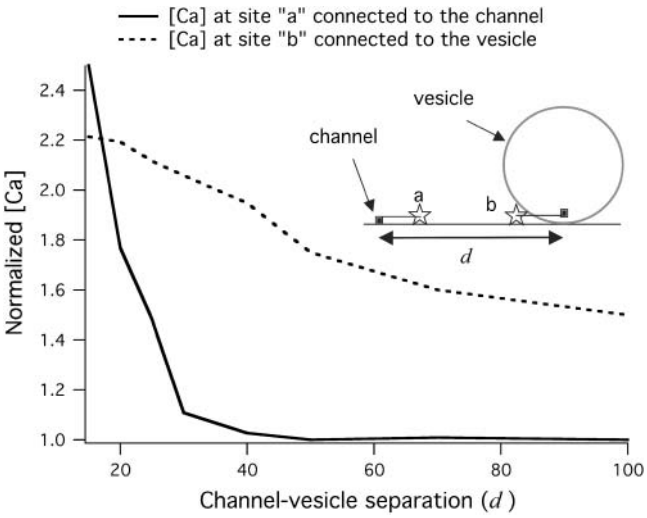

FIGURE 7 The steady-state [Ca] at two sites 10 nm from the vesicle or 10 nm from the channel as a function of channel-vesicle separation.

between the channel and the vesicle, 10 nm from the channel, as we vary d from 15 to 100 nm. The solid line in Fig. 7 shows these [Ca] values scaled to the corresponding [Ca] in the absence of the vesicle. This scaled [Ca] starts from 2.5 and falls rapidly to 1 as d becomes comparable to the vesicle diameter. This result shows that the vesicle only distorts the [Ca] profile in its vicinity. The dashed line in Fig. 7 shows normalized [Ca] at a point between the channel and the vesicle, 10 nm from the vesicle, as we vary d from 15 to 100 nm. This scaled [Ca] starts at 2.2 and decreases slowly to ~1.5 at 100-nm separation. So, even for distant separations between the channel and the vesicle, the [Ca] distortion in the vicinity of the vesicle is significant. The effect of the vesicle on the [Ca] in its vicinity is weakly dependent on the Ca^{2+} channel-vesicle separation. The distortion of the [Ca] profile is maximal for the region of space between the Ca^{2+} channel and the vesicle when their separation is smaller than vesicle diameter.

This separation dependence suggests that the effect of a second vesicle on [Ca] in the vicinity of a vesicle should not be significant. To test this idea directly, we show in Fig. 8 the image plots of [Ca] close to the active zone membrane for two different arrangements of a channel and two vesicles. In both cases we assume the vesicles are in contact with one another (50 nm apart). In Fig. 8 *A* the channel is 20 nm on the side of the first vesicle on a line perpendicular to the row of two vesicles. This arrangement of the channels resembles the frog neuromuscular junction active zone, where vesicles are docked in two parallel rows and Ca^{2+} channels are located between the rows (Harlow et al., 2001). In this case the channel and the second vesicle are separated by ~54 nm. The presence of the second vesicle does not alter [Ca] at the midpoint between the channel and the first vesicle significantly, since it is not very close. In Fig. 8 *B* the channel is situated between the two vesicles, where it is 20-nm away from the first vesicle and 30-nm away from the second one. In this case the presence of the second vesicle increases the [Ca] at the midpoint between the channel and the first vesicle by ~6%.

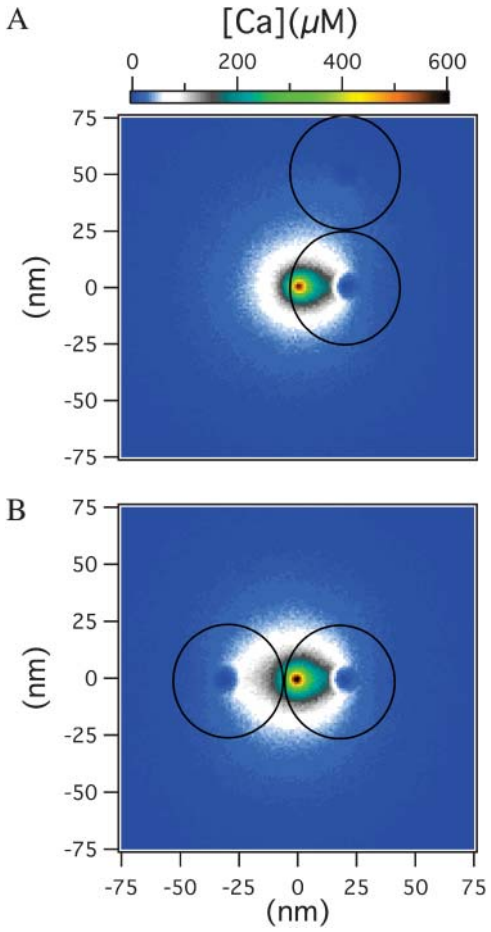

FIGURE 8 The image plot of the [Ca] in the plane $z = 0$ (x,y cross section of Fig. 1 *A*) after a sustained opening of the channel for 0.3 ms in the presence of two side-by-side docked vesicles in two arrangements. (*A*) Channel is situated 20 nm from the docking point of the first vesicle perpendicular to the direction of the row of two vesicles. (*B*) Channel is situated 20 nm from the docking point of the first vesicle between the two vesicles.

Spatial arrangement of release machinery and release probability

As we saw in the last section, the steady-state [Ca] around the vesicle varies significantly. Since release is highly nonlinear in [Ca], release probability should depend critically on the position of Ca^{2+}-sensor(s). Here we vary the position of the Ca^{2+}-sensor and compare the release probability for two representative release models. Models 1 and 2 have low and high affinity for Ca^{2+}, respectively (Heidelberger et al., 1994; Bollmann et al., 2000). For calculating release probabilities, we produce a Ca^{2+} current of 0.3 pA into the terminal for 0.3 ms, and see if the release machinery reaches the fusion step by 0.6 ms after the closure of the channel. Release rate after 0.6 is close to 0, since there are almost no Ca^{2+} ions left in the system. We repeat this 1000 times for each choice of position for the Ca^{2+}-sensor. Release probability for a single vesicle for one channel opening is the fraction of the Monte Carlo trials for which fusion was achieved.

The illustration in Fig. 9 *A* shows our choices for the location of the Ca^{2+}-sensor with respect to the channel and the vesicle. The release probabilities with different choices of parameters for release models 1 and 2 are shown in Fig. 9, *B* and *C*, respectively. The release probabilities for model 1 (low affinity) are dramatically lower than those for model 2 (high affinity). For example, if we locate the sensor at point *a*, the release probability is 0.057 for model 1 compared to 0.99 for model 2. If we position the Ca^{2+} sensor on the far side of the vesicle the release probability for model 1 is zero (data not shown) and very small for model 2 (e.g., for point *e*, it is 0.02). Using model 1, decreasing the distance between the Ca^{2+} sensor and the channel from 10 nm to 5 nm (from

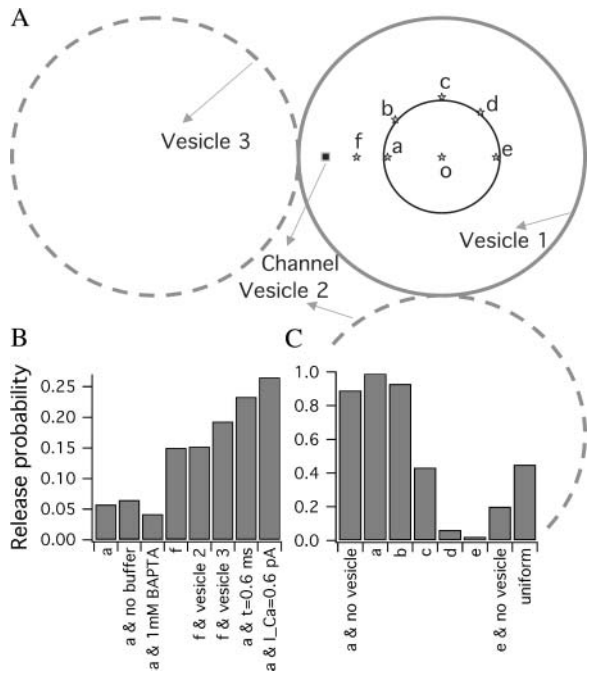

FIGURE 9 (*A*) Schematic view of the arrangement of Ca^{2+} channel and the vesicle(s) and the Ca^{2+}-sensor sites of the release machinery. The cartoon shows the plane $z = 0$ (x,y cross section of Fig. 1 *A*). Release probability for model 1 (*B*) and model 2 (*C*) for different choices of Ca^{2+}-sensor site position (from *a* to *e*). 0.5 mM mobile buffer with properties shown in Table 1 is present unless mentioned. Ca^{2+} Current duration (t) is 0.3 ms and current size (I_Ca) is 0.3 pA, unless otherwise noted. Vesicle 1 is present, unless otherwise noted.

a to *f*) increases release probability threefold (from 0.057 to 0.15; see Fig. 9 *B*). The presence of a second vesicle does not have a large effect on [Ca] at locations near the first vesicle and, as a result, on the release probability, particularly if the second vesicle is far from the Ca^{2+}-sensor site. For example, the presence of vesicle 3 increases the release probability by 25%, but vesicle 2, which is located further from the sensor site, does not have any significant effect. So other diffusional barriers like intracellular organelles should not have an important effect on the release.

In general mobile buffers may have a large effect on release since they significantly reduce the overlap of the Ca^{2+} channel microdomains (Adler et al., 1991; Burrone et al., 2002). This is not the case in our simulations, since we have focused on a single channel colocalized with a vesicle. The endogenous buffer used in our simulations does not have a large effect on the [Ca] in the vicinity of the channel. Because of the close proximity between Ca^{2+} channel and the Ca^{2+}-sensor, release probability is not significantly reduced in the presence of the buffer (Fig. 9 *B*). For example, removing all endogenous buffers only increases release probability ~10% (0.065 compared to 0.057). Substantially increasing endogenous buffer strength by increasing the capacity 20-fold (1 mM of a fast high-affinity buffer like BAPTA, $K_d = 0.22\ \mu M$ with diffusion coefficient similar to Ca^{2+}) reduces the release probability by only 30%.

Release probability is highly dependent upon the total Ca^{2+} influx but is much less sensitive to the actual form of the Ca^{2+} current. In model 1, increasing the total influx by a factor of 2, enhances release probability by approximately a factor of 5. This is a direct consequence of high cooperativity of Ca^{2+} for release. But, whether the increase in Ca^{2+} influx is in its duration (0.3–0.6 ms) or its size (0.3–0.6 pA), the resulting release probability is approximately the same (0.233 compared to 0.265). The total number of Ca^{2+} ions that pass by vicinity of the Ca^{2+}-sensor, and have the chance to react with it, is just a function of total influx (this is true if the buffer is far from saturation). If the dissociation time constant (one over the off-rate of the binding site) is comparable or longer than the duration of the current, then, if a Ca^{2+} ion binds to the sensor, it probably stays for the whole duration of the current. As a result, the dependence on the form of the current is weak. This justifies the use of a simple form for the Ca^{2+} current.

Using model 2, ignoring the effect of the vesicle on the spatial distribution of [Ca] decreases the release probability when the Ca^{2+}-sensor is located at point *a* and increases it when the Ca^{2+}-sensor is located at point *e* (Fig. 9 *C*). Moving the Ca^{2+}-sensor around the vesicle from *a* to *e* decreases the release probability by 50-fold (from 0.99 to 0.02). This is a direct consequence of changes in [Ca] around the vesicle. If we assume the five binding sites are on different sensor molecules distributed uniformly around the vesicle (the first one at *a* and one at every 72° around the vesicle) the release probability for model 2 is ~0.45. The release probability is strongly dependent on the position of the Ca^{2+}-sensor around the vesicle relative to the channel.

DISCUSSION

Using Monte Carlo simulations we show that a synaptic vesicle colocalized with a Ca^{2+} channel modifies the Ca^{2+} microdomain. This could have important consequences for neurotransmitter release, depending on the microgeometry of the vesicle, Ca^{2+} channel, and Ca^{2+}-sensor complex.

Our knowledge of the geometry of different components of the release machinery is growing quickly but is still far from complete. We do not know the exact positioning of different proteins relative to the synaptic vesicle and the Ca^{2+} channel. We also do not know if they have a flexible geometry, if they are highly constrained, or to what extent their relative structure can be modulated (Stanley et al., 2003). Although release seems to arise from the cooperative action of several Ca^{2+} channels in some synapses (Borst and Sakmann, 1996), there is good evidence for release evoked by one or a few channels opening in other synapses (Augustine et al., 1991; Stanley, 1993; Mulligan et al., 2001; Wachman et al., 2004). This wide range of Ca^{2+} channel cooperativity might be attributed to, or influenced

by, the particular active zone organization found at various central and peripheral synapses (Stanley, 1997). Some synapses, such as the squid giant synapse and most central synapses, possess seemingly random loose clusters of release sites (Pumplin and Reese, 1978). Some other synapses, such as vertebrate skeletal neuromuscular junctions, have an ordered release site organization. This is usually in the form of two rows of vesicles with associated parallel rows of Ca^{2+} channels (Heuser et al., 1974).

To explore the effect of the blocking of Ca^{2+} diffusion by the vesicle, we focused on a single channel and its colocalized vesicle. We assumed the channel is 20 nm from the vesicle. This is consistent with the high-resolution morphological studies in neuromuscular junctions (Heuser et al., 1979; Harlow et al., 2001; Stanley et al., 2003) and also the size of SNARE complex (Sutton et al., 1998), if one assumes physical connections between the release machinery and the Ca^{2+} channel (Sheng et al., 1998; Jarvis and Zamponi, 2001). We assumed the Ca^{2+}-sensor(s) are somewhere around the contact point of vesicle and the membrane at a radius of 10 nm. Although the Ca^{2+}-sensor(s) could be a bit further away from the contact point, the size of the Ca^{2+}-sensor candidate, the synaptotagmin molecule (Fernandez et al., 2001), makes a closer distance to the contact point unlikely.

A systematic understanding of neurotransmitter release demands detailed knowledge of the spatiotemporal dynamics of Ca^{2+} ions in the presynaptic terminal. Unfortunately, present experimental techniques cannot directly resolve changes in intracellular [Ca] at nanometer spatial and microsecond temporal scales, so mathematical modeling of the Ca^{2+} diffusion-reaction remains a useful method available to address this important problem. For this study we implemented a Monte Carlo simulation of the Ca^{2+} and mobile buffer diffusion-reaction to look at the role of the geometry of the active zone. This method is efficient to look at problems with complicated boundary geometry and to resolve concentration changes at the nanometer level.

In the context of neurotransmitter release, the effect of diffusional barriers has been examined for simplified geometries (Kennedy et al., 1999; Kits et al., 1999; Glavinovic and Rabie, 2001). These studies have shown that barriers can affect the spatiotemporal distribution of Ca^{2+} and bound buffers. Barriers limit the effect of mobile buffers and can enhance saturation of fixed buffers. Here we extend the previous studies to a case in which we use the actual geometry of a vesicle and its position adjacent to the plasmalemma.

The presence of a synaptic vesicle in the vicinity of the channel has a large effect on the Ca^{2+} microdomain profile. It alters the average path for the Ca^{2+} ions to reach a specific point around the vesicle. For a Ca^{2+} current of 0.3 pA and 0.5 mM of mobile buffer, the steady-state [Ca] 10 nm from the channel in the absence of vesicle is $\sim$100 μM. A docked vesicle increases this steady-state [Ca] to $>$200 μM by blocking the escape routes of Ca^{2+} molecules. The [Ca] is greater on the channel side of the vesicle (and lower on the opposite side) than the corresponding [Ca] in the absence of the vesicle. These effects are dependent upon the distance from the vesicle, the extent of separation of the vesicle from the presynaptic membrane, the distance between the channel and the vesicle, and the size of the vesicle. A tightly docked vesicle is more effective in blocking the free diffusion of Ca^{2+}, and the effect is maximal in the vicinity of the vesicle. The blocking effect remains, although to a smaller degree, even for channel-vesicle separations larger than vesicle diameter. We find that, as the position of the Ca^{2+}-sensor sites varies around the vesicle, the standing [Ca] that they experience changes by up to 13-fold. The blocking effects of the vesicle do not depend strongly on the magnitude of Ca^{2+} current or the buffer concentration used.

Other diffusional barriers in presynaptic terminal like cytoskeleton and other organelles modify the [Ca] in their vicinity but do not affect the [Ca] sensed for release. A rule of thumb is that any barrier can change the [Ca] profile around it up to a distance comparable to its dimensions. So although some structural proteins can be located nanometers away from the release machinery, they are not wide enough to affect free Ca^{2+} diffusion. Also, internal organelles like mitochondria, although large, are not close enough to the release machinery. In this sense, a docked synaptic vesicle has a unique effect in modifying the [Ca] sensed for the release, since it is big and close enough to do so. For similar reasons the effect of undocked vesicles or other docked vesicles located at a distance greater than the diameter of the vesicle is not expected to be significant. So, the ongoing active geometrical changes that are taking place by the docking and fusion of the neighboring vesicles would not be expected to influence significantly the [Ca] profile for a given vesicle. In amphibian neuromuscular junctions, where the active zone consists of two ordered rows of tightly docked vesicles, the vesicles and the presynaptic membrane active zone ridge collectively form a restricted physical space between them (Harlow et al., 2001). Interestingly, the Ca^{2+} channels are believed to reside in this region (Heuser et al., 1979; Pumplin et al., 1981). Thus, in this case the vesicles could have a significant effect on the spatial [Ca] distribution.

Our results on the modifications of ion channel microdomains by diffusional barriers are general and are applicable to other biological systems where channels open into restricted spaces. For example, in striated muscle fibers, the Ca^{2+} microdomain of the Ca^{2+} channels would be affected by the narrow junctional space between the T-tubule and sarcoplasmic reticulum membranes ($\sim$35 nm) (Bers, 2001). In this case, since the escape routes for Ca^{2+} ions are reduced, the steady-state [Ca] should reach higher levels compared to an unrestricted Ca^{2+} microdomain. Another example of Ca^{2+} domains in a restricted space for which our results may be relevant is the release of calcium from endoplasmic reticulum near the plasma membrane.

There is a growing evidence for the importance of the single Ca^{2+} domains in release (Wachman et al., 2004). The blocking effect of the vesicle on release is maximal for a single channel-mediated release scenario. The release probability of a vesicle during a brief opening of a nearby Ca^{2+} channel is highly sensitive to the spatial position of the Ca^{2+}-sensor relative to the vesicle and the channel. For example, for a high-affinity release model (model 2), a uniform distribution of the binding sites around the vesicle gives rise to a release probability of ~0.45. However, using the same model the release probability can vary from 0.02 to 0.99 depending on the position of the Ca^{2+}-sensor. The lowest release probability corresponds to the unlikely situation of having all the binding sites on the far side of the vesicle from the channel. This large range arises because the [Ca] gradient close to a Ca^{2+} channel is very steep, the presence of the vesicle produces additional sharpening of the [Ca] profile, and also because release is highly cooperative for Ca^{2+}. As a result any flexibility in the position of the Ca^{2+} sensors would be expected to produce heterogeneity of release probability. Some synapses, like the calyx of Held, are believed to have a pool of vesicles with very heterogeneous release probabilities (Rosenmund et al., 1993; Sakaba and Neher, 2001). Also, different synapses operate with a wide range of release probabilities, where even synapses made by a single neuron can have very different release probabilities (Rozov et al., 2001). In addition to the possibility of the existence of different types of Ca^{2+} sensors, variations in the geometry of the active zone, particularly in the channel-vesicle separation is thought to be important (Meinrenken et al., 2002). We hypothesize that variation in the position of the Ca^{2+} sensor for release is an additional mechanism that could be used to produce heterogeneity of release within a synapse or between different synapses.

Although a systematic study of the geometrical effects for multiple channels-mediated release is beyond the scope of this study, some of the ideas presented here can be generalized. The vesicle will modify [Ca] sensed by the Ca^{2+} sensor. Since the increase in [Ca] on the channel side of the vesicle is higher than the reduction in the far side of the vesicle due to blocking (Fig. 6), on average the [Ca] achieved in the vicinity of the vesicle will be higher than that which is estimated from modeling studies that ignore the vesicle. If multiple channels open equidistantly all around the vesicle, the [Ca] achieved at the vesicle is expected to be relatively uniform. But if all the channels are situated on one side of the vesicle (e.g., amphibian neuromuscular junctions) or if one of the open channels is relatively closer to the vesicle than others, some level of variation of [Ca] around the vesicle is expected. The vesicle could also limit access of Ca^{2+} from some of the channels to the sensor. As a result the vesicle may reduce the number of channels contributing to the release, thus it could modify the channel cooperativity of the release.

Finally, our simulations show that, if release is not saturated (low affinity, e.g., model 1), small spatial movements (~5 nm) of the Ca^{2+}-sensor sites cause significant changes in release probability (up to threefold). A recent study in chromaffin cells showed an activity dependent reduction in separation of docked dense-core vesicles and Ca^{2+} entry sites, which was suggested as a new mechanism for stimulation-dependent facilitation of release (Becherer et al., 2003). There is also evidence suggesting the Ca^{2+}-dependent interactions between some of the SNARE proteins and Ca^{2+} channels (Jarvis and Zamponi, 2001). These interactions could bring the Ca^{2+}-sensor closer to the channel after introduction of Ca^{2+} ions during an action potential, and therefore, increase the release probability for subsequent action potentials. Similar to the idea presented by Becherer et al. (2003) this would represent a new mechanism for Ca^{2+}-dependent synaptic plasticity, which only requires the slight movement of the Ca^{2+}-sensor molecule associated with the vesicle toward the Ca^{2+} channel rather than the vesicle itself.

We thank Michael Wortis, Michael Plischke, Timothy Murphy, Harold Atwood, James Winslow, Glen Tibbits, Ed Chapman, Daniel Vernon, and Colin Demill for helpful discussions and Gerald Lim for advice on the presentation of the isoconcentration data.

This study was supported by a grant from the Natural Sciences and Engineering Research Council of Canada (RGPIN121698).

REFERENCES

Adler, E. M., G. J. Augustine, S. N. Duffy, and M. P. Charlton. 1991. Alien intracellular calcium chelators attenuate neurotransmitter release at the squid giant synapse. *J. Neurosci.* 11:1496–1507.

Andreucci, D., P. Bisegna, G. Caruso, H. E. Hamm, and E. DiBenedetto. 2003. Mathematical model of the spatio-temporal dynamics of second messengers in visual transduction. *Biophys. J.* 85:1358–1376.

Augustine, G. J. 2001. How does calcium trigger neurotransmitter release? *Curr. Opin. Neurobiol.* 11:320–326.

Augustine, G. J., E. M. Adler, and M. P. Charlton. 1991. The calcium signal for transmitter secretion from presynaptic nerve terminals. *Ann. N. Y. Acad. Sci.* 635:365–381.

Bai, J., C. T. Wang, D. A. Richards, M. B. Jackson, and E. R. Chapman. 2004. Fusion pore dynamics are regulated by synaptotagmin-tSNARE interactions. *Neuron.* 41:929–942.

Bartol, T. M., Jr., B. R. Land, E. E. Salpeter, and M. M. Salpeter. 1991. Monte Carlo simulation of miniature endplate current generation in the vertebrate neuromuscular junction. *Biophys. J.* 59:1290–1307.

Becherer, U., T. Moser, W. Stuhmer, and M. Oheim. 2003. Calcium regulates exocytosis at the level of single vesicles. *Nat. Neurosci.* 6: 846–853.

Bennett, M. R., L. Farnell, and W. G. Gibson. 2000a. The probability of quantal secretion near a single calcium channel of an active zone. *Biophys. J.* 78:2201–2221.

Bennett, M. R., L. Farnell, and W. G. Gibson. 2000b. The probability of quantal secretion within an array of calcium channels of an active zone. *Biophys. J.* 78:2222–2240.

Bennett, M. R., W. G. Gibson, and J. Robinson. 1997. Probabilistic secretion of quanta and the synaptosecretosome hypothesis: evoked

release at active zones of varicosities, boutons, and endplates. *Biophys. J.* 73:1815–1829.

Bers, D. M. 2001. Excitation-Contraction Coupling and Cardiac Contractile Force. Kluwer Academic Publishers, Dordrecht, The Netherlands.

Bollmann, J. H., B. Sakmann, and J. G. Borst. 2000. Calcium sensitivity of glutamate release in a calyx-type terminal. *Science.* 289:953–957.

Borst, J. G., and B. Sakmann. 1996. Calcium influx and transmitter release in a fast CNS synapse. *Nature.* 383:431–434.

Burrone, J., G. Neves, A. Gomis, A. Cooke, and L. Lagnado. 2002. Endogenous calcium buffers regulate fast exocytosis in the synaptic terminal of retinal bipolar cells. *Neuron.* 33:101–112.

Chad, J. E., and R. Eckert. 1984. Calcium domains associated with individual channels can account for anomalous voltage relations of Ca^{2+}-dependent responses. *Biophys. J.* 45:993–999.

Chapman, E. R. 2002. Synaptotagmin: a Ca^{2+} sensor that triggers exocytosis? *Nat. Rev. Mol. Cell Biol.* 3:498–508.

Cooper, R. L., J. L. Winslow, C. K. Govind, and H. L. Atwood. 1996. Synaptic structural complexity as a factor enhancing probability of calcium-mediated transmitter release. *J. Neurophysiol.* 75:2451–2466.

Dodge, F. A., Jr., and R. Rahamimoff. 1967. Co-operative action of calcium ions in transmitter release at the neuromuscular junction. *J. Physiol.* 193:419–432.

Fernandez, I., D. Arac, J. Ubach, S. H. Gerber, O. Shin, Y. Gao, R. G. Anderson, T. C. Sudhof, and J. Rizo. 2001. Three-dimensional structure of the synaptotagmin 1 C2B-domain: synaptotagmin 1 as a phospholipid binding machine. *Neuron.* 32:1057–1069.

Gil, A., J. Segura, J. A. Pertusa, and B. Soria. 2000. Monte Carlo simulation of 3-D buffered Ca^{2+} diffusion in neuroendocrine cells. *Biophys. J.* 78:13–33.

Glavinovic, M. I., and H. R. Rabie. 2001. Monte Carlo evaluation of quantal analysis in the light of Ca^{2+} dynamics and the geometry of secretion. *Pflugers Arch.* 443:132–145.

Han, X., C. T. Wang, J. Bai, E. R. Chapman, and M. B. Jackson. 2004. Transmembrane segments of syntaxin line the fusion pore of Ca^{2+}-triggered exocytosis. *Science.* 304:289–292.

Harlow, M. L., D. Ress, A. Stoschek, R. M. Marshall, and U. J. McMahan. 2001. The architecture of active zone material at the frog's neuromuscular junction. *Nature.* 409:479–484.

Heidelberger, R., C. Heinemann, E. Neher, and G. Matthews. 1994. Calcium dependence of the rate of exocytosis in a synaptic terminal. *Nature.* 371:513–515.

Heuser, J. E., T. S. Reese, M. J. Dennis, Y. Jan, L. Jan, and L. Evans. 1979. Synaptic vesicle exocytosis captured by quick freezing and correlated with quantal transmitter release. *J. Cell Biol.* 81:275–300.

Heuser, J. E., T. S. Reese, and D. M. Landis. 1974. Functional changes in frog neuromuscular junctions studied with freeze-fracture. *J. Neurocytol.* 3:109–131.

Holcman, D., and J. I. Korenbrot. 2004. Longitudinal diffusion in retinal rod and cone outer segment cytoplasm: the consequence of cell structure. *Biophys. J.* 86:2566–2582.

Hua, Y., and R. H. Scheller. 2001. Three SNARE complexes cooperate to mediate membrane fusion. *Proc. Natl. Acad. Sci. USA.* 98:8065–8070.

Jarvis, S. E., and G. W. Zamponi. 2001. Interactions between presynaptic Ca^{2+} channels, cytoplasmic messengers and proteins of the synaptic vesicle release complex. *Trends Pharmacol. Sci.* 22:519–525.

Kennedy, K. M., S. T. Piper, and H. L. Atwood. 1999. Synaptic vesicle recruitment for release explored by Monte Carlo stimulation at the crayfish neuromuscular junction. *Can. J. Physiol. Pharmacol.* 77:634–650.

Kits, K. S., T. A. de Vlieger, B. W. Kooi, and H. D. Mansvelder. 1999. Diffusion barriers limit the effect of mobile calcium buffers on exocytosis of large dense cored vesicles. *Biophys. J.* 76:1693–1705.

Llinas, R., I. Z. Steinberg, and K. Walton. 1981. Relationship between presynaptic calcium current and postsynaptic potential in squid giant synapse. *Biophys. J.* 33:323–351.

Llinas, R., M. Sugimori, and R. B. Silver. 1992. Microdomains of high calcium concentration in a presynaptic terminal. *Science.* 256:677–679.

Matsumoto, M., and T. Nishimura. 1998. Mersenne Twister: A 623-dimensionally equidistributed uniform pseudorandom number generator. *ACM Trans. Model. Comput. Sim.* 8:3–30.

Matthews, G. 1996. Neurotransmitter release. *Annu. Rev. Neurosci.* 19: 219–233.

Meinrenken, C. J., J. G. Borst, and B. Sakmann. 2002. Calcium secretion coupling at calyx of held governed by nonuniform channel-vesicle topography. *J. Neurosci.* 22:1648–1667.

Mulligan, S. J., I. Davison, and K. R. Delaney. 2001. Mitral cell presynaptic Ca^{2+} influx and synaptic transmission in frog amygdala. *Neuroscience.* 104:137–151.

Nakatani, K., C. Chen, and Y. Koutalos. 2002. Calcium diffusion coefficient in rod photoreceptor outer segments. *Biophys. J.* 82:728–739.

Naraghi, M., and E. Neher. 1997. Linearized buffered Ca^{2+} diffusion in microdomains and its implications for calculation of [Ca] at the mouth of a calcium channel. *J. Neurosci.* 17:6961–6973.

Olveczky, B. P., and A. S. Verkman. 1998. Monte Carlo analysis of obstructed diffusion in three dimensions: application to molecular diffusion in organelles. *Biophys. J.* 74:2722–2730.

Pumplin, D. W., and T. S. Reese. 1978. Membrane ultrastructure of the giant synapse of the squid *Loligo pealei*. *Neuroscience.* 3:685–696.

Pumplin, D. W., T. S. Reese, and R. Llinas. 1981. Are the presynaptic membrane particles the calcium channels? *Proc. Natl. Acad. Sci. USA.* 78:7210–7213.

Raichl, L. E. 1980. A Modern Course in Statistical Mechanics. University of Texas Press, Austin, TX.

Rosenmund, C., J. D. Clements, and G. L. Westbrook. 1993. Nonuniform probability of glutamate release at a hippocampal synapse. *Science.* 262:754–757.

Rozov, A., N. Burnashev, B. Sakmann, and E. Neher. 2001. Transmitter release modulation by intracellular Ca^{2+} buffers in facilitating and depressing nerve terminals of pyramidal cells in layer 2/3 of the rat neocortex indicates a target cell-specific difference in presynaptic calcium dynamics. *J. Physiol.* 531:807–826.

Sabatini, B. L., and W. G. Regehr. 1996. Timing of neurotransmission at fast synapses in the mammalian brain. *Nature.* 384:170–172.

Sakaba, T., and E. Neher. 2001. Quantitative relationship between transmitter release and calcium current at the calyx of held synapse. *J. Neurosci.* 21:462–476.

Sala, F., and A. Hernandez-Cruz. 1990. Calcium diffusion modeling in a spherical neuron. Relevance of buffering properties. *Biophys. J.* 57: 313–324.

Saxton, M. J. 1994. Anomalous diffusion due to obstacles: a Monte Carlo study. *Biophys. J.* 66:394–401.

Schneggenburger, R., and E. Neher. 2000. Intracellular calcium dependence of transmitter release rates at a fast central synapse. *Nature.* 406: 889–893.

Segura, J., A. Gil, and B. Soria. 2000. Modeling study of exocytosis in neuroendocrine cells: influence of the geometrical parameters. *Biophys. J.* 79:1771–1786.

Sheng, Z. H., R. E. Westenbroek, and W. A. Catterall. 1998. Physical link and functional coupling of presynaptic calcium channels and the synaptic vesicle docking/fusion machinery. *J. Bioenerg. Biomembr.* 30:335–345.

Simon, S. M., and R. R. Llinas. 1985. Compartmentalization of the submembrane calcium activity during calcium influx and its significance in transmitter release. *Biophys. J.* 48:485–498.

Smith, G. D. 1996. Analytical steady-state solution to the rapid buffering approximation near an open Ca^{2+} channel. *Biophys. J.* 71:3064–3072.

Stanley, E. F. 1993. Single calcium channels and acetylcholine release at a presynaptic nerve terminal. *Neuron.* 11:1007–1011.

Stanley, E. F. 1997. The calcium channel and the organization of the presynaptic transmitter release face. *Trends Neurosci.* 20:404–409.

Stanley, E. F., T. S. Reese, and G. Z. Wang. 2003. Molecular scaffold reorganization at the transmitter release site with vesicle exocytosis or botulinum toxin C1. *Eur. J. Neurosci.* 18:2403–2407.

Stern, M. D. 1992. Buffering of calcium in the vicinity of a channel pore. *Cell Calcium.* 13:183–192.

Stewart, B. A., M. Mohtashami, W. S. Trimble, and G. L. Boulianne. 2000. SNARE proteins contribute to calcium cooperativity of synaptic transmission. *Proc. Natl. Acad. Sci. USA.* 97:13955–13960.

Sudhof, T. C. 1995. The synaptic vesicle cycle: a cascade of protein-protein interactions. *Nature.* 375:645–653.

Sutton, R. B., D. Fasshauer, R. Jahn, and A. T. Brunger. 1998. Crystal structure of a SNARE complex involved in synaptic exocytosis at 2.4 Å resolution. *Nature.* 395:347–353.

Tang, Y., T. Schlumpberger, T. Kim, M. Lueker, and R. S. Zucker. 2000. Effects of mobile buffers on facilitation: experimental and computational studies. *Biophys. J.* 78:2735–2751.

Ubach, J., X. Zhang, X. Shao, T. C. Sudhof, and J. Rizo. 1998. Ca^{2+} binding to synaptotagmin: how many Ca^{2+} ions bind to the tip of a C2-domain? *EMBO J.* 17:3921–3930.

Wachman, E. S., R. E. Poage, J. R. Stiles, D. L. Farkas, and S. D. Meriney. 2004. Spatial distribution of calcium entry evoked by single action potential within the presynaptic active zone. *J. Neurosci.* 24:2877–2885.

Wagner, J., and J. Keizer. 1994. Effects of rapid buffers on Ca^{2+} diffusion and Ca^{2+} oscillations. *Biophys. J.* 67:447–456.

Weber, T., B. V. Zemelman, J. A. McNew, B. Westermann, M. Gmachl, F. Parlati, T. H. Sollner, and J. E. Rothman. 1998. SNAREpins: minimal machinery for membrane fusion. *Cell.* 92:759–772.

Westenbroek, R. E., J. W. Hell, C. Warner, S. J. Dubel, T. P. Snutch, and W. A. Catterall. 1992. Biochemical properties and subcellular distribution of an N-type calcium channel alpha 1 subunit. *Neuron.* 9:1099–1115.

Westenbroek, R. E., T. Sakurai, E. M. Elliott, J. W. Hell, T. V. Starr, T. P. Snutch, and W. A. Catterall. 1995. Immunochemical identification and subcellular distribution of the alpha 1A subunits of brain calcium channels. *J. Neurosci.* 15:6403–6418.

Winslow, J. L., S. N. Duffy, and M. P. Charlton. 1994. Homosynaptic facilitation of transmitter release in crayfish is not affected by mobile calcium chelators: implications for the residual ionized calcium hypothesis from electrophysiological and computational analyses. *J. Neurophysiol.* 72:1769–1793.

Yamada, W. M., and R. S. Zucker. 1992. Time course of transmitter release calculated from simulations of a calcium diffusion model. *Biophys. J.* 61:671–682.

Zucker, R. S. 1993. Calcium and transmitter release. *J. Physiol. (Paris).* 87:25–36.

Zucker, R. S., and A. L. Fogelson. 1986. Relationship between transmitter release and presynaptic calcium influx when calcium enters through discrete channels. *Proc. Natl. Acad. Sci. USA.* 83:3032–3036.